energies

MDPI

Review

Efficient Stabilization of Mono and Hybrid Nanofluids

Sylwia Wciślik

Department of Piped Utility Systems, Faculty of Environmental, Geomatic and Energy Engineering, Kielce University of Technology, Aleja Tysiaclecia Panstwa Polskiego 7, 25-314 Kielce, Poland; sylwiazw@tu.kielce.pl

Received: 23 June 2020; Accepted: 16 July 2020; Published: 23 July 2020

Abstract: Currently; the transfer of new technologies makes it necessary to also control heat transfer in different industrial processes—both in practical and research—applications. Not so long ago water and ethylene glycol were the most frequently used media in heat transfer. However, due to their relatively low thermal conductivity, they cannot provide the fast and effective heat transfer necessary in modern equipment. To improve the heat transfer rate different additives to the base liquid are sought, e.g., nanoadditives that create mono and hybrid nanofluids with very high thermal conductivity. The number of scientific studies and publications concerning hybrid nanofluids is growing, although they still represent a small percentage of all papers on nanofluids (in 2013 it was only 0.6%, and in 2017—ca. 3%). The most important point of this paper is to discuss different ways of stabilizing nanofluids, which seems to be one of the most challenging tasks in nanofluid treatment. Other future challenges concerning mono and hybrid nanofluids are also thoroughly discussed. Moreover, a quality assessment of nanofluid preparation is also presented. Thermal conductivity models are specified as well and new representative mono and hybrid nanofluids are proposed.

Keywords: hybrid nanofluid; thermal conductivity; Brownian motions; ultrasonication; one- and two-step colloid stability method; sedimentation

1. Introduction

Fluids currently used in industrial installations and thermal flow systems are very often modified with different types of additives [1] in order to make them achieve the best possible thermodynamic parameters, and thus to improve heat transfer conditions. In 1995, researchers from the Argonne National Laboratory proposed for the first time the practical use of copper nanoparticles dispersed in water—the fluid which is most commonly used in all sorts of heat exchangers—in order to improve the thermal conductivity. However, the origin of nanotechnology and nanoscience definition/concept reaches back to 1959, when an American Nobel laureate—Richard Feynman— proposed a new theory of quantum electrodynamics. Norio Taniguchi, who presented the basic concept of 'nano-technology' in 1974 during the International Conference on Production Engineering in Japan is also thought to be a pioneer of nanotechnology as a science [2]. The chronological development of the field is summarized in Table 1.

Table 1. Most important historical events of nanoadditives and nanofluids in heat transfer applications.

1873	Maxwell [3] proposes the innovative idea of adding solid particles to heat transfer fluids to rise their thermal conductivity thermodynamic parameter.
1881	Maxwell published academic and experimental papers of the effective thermal conductivity of dispersions with millimetre and micrometer-sized solid particles.
1951	Development of ferrofluids as intelligent nanofluids (Bozorth [4])
1959	Richard Feynman proposes a new theory of quantum electrodynamics and the technical directions of nanoscience were defined.
1974	Norio Taniguchi presents in Japan the basic concept of 'nanotechnology'.
1978	Suggestions to produce nanophase powders from the vapor phase directly into a flowing low vapor pressure fluid fail due to problems in subsequently separating the dry particles (Akoh et al. [5]).
1986	Drexlers gives the idea of molecular nanotechnology and claims Feynman theory.
1989–1994	Advanced fluids for industrial applications—including district heating and cooling systems—are developed by researchers from the Argonne National Laboratory. The need for nanoscale additives to prevent clogging problems in heat exchangers was delineated.
	Confirmation that the thermal, mechanical, optical, magnetic, and electrical properties of nanoadditives and nanofluids are much better in comparison to those of the typical fluids used in industrial applications. The relatively high surface-area-to-volume ratio of nanoadditives that is due to the high percent of constituent atoms that reside at the grain boundaries was used by material scientists and engineers alike (e.g., Duncan and Rouvray, [6]; Siegel and Estman, [7]).
	Development of physical gas-phase condensation or chemical synthesis techniques for the production of nanopowders with average particle sizes in the 10 nm range.
1963–1992	Development a third technique for nanophase material generation by condensation of metal vapors during rapid expansion in a supersonic nozzle (e.g., Hill, et al., [8]; Andres, et al., [9]; Brown, et al., [10]).
1995	Choi and Eastman propose for the first time the practical use of copper nanoparticles dispersed in water [11].
2000–	Development of mono and hybrid nanofluids for heat transfer applications (problems and techniques of stabilization, coagulation and clustering of multi-sized nanocomposites, heat transfer models, thermal and rheological properties upgrading) and other problems described in the following sections of this review.

To this day, this discipline is growing and is used in many sectors of the economy, thermotechnology (mini-channels [12,13], extended surfaces as fins [14,15], phase change materials—PCMs [16] and so on), solar technology [17], electronics [18], as well as in chemical industry, agriculture, [19] and even medicine [20].

1.1. Types of Conventional Nanoadditives

The name nanofluids applies to colloids which contain solid particles sized from 1 to 100 nm. These are called nanoadditives and are divided into three basic groups: metallic, oxide and carbon (SWNT, DWNT, MWCNT or single-, double-, multi- wall carbon nanotubes respectively), as shown and classified in Figure 1.

Metal nitrides and carbides constitute separate groups of inorganic chemicals.

1.2. Nanocomposites

If nanoliquids are to be used in technological processes, it is important to decide on the appropriate selection of the nanoadditive (depending on required heating/cooling effects) and its concentration. This leads to an increase in the density of dissipated heat and accelerates the processes of thermal treatment processes. For this purpose, intensified research works on hybrid nanofluids have been

carried out recently. These are substances (the so-called nanocomposites), in which at least two types of nano-size particles (in nanometer range) are dispersed, and their physical and chemical (particularly thermal and rheological [21]) properties are specific and practically unattainable without this combination. Depending on the type of nanocomposite used, hybrid nanofluids are divided into three basic groups, which is for instance shown in Figure 2. The methods of synthesising more than 25 nanocomposites are also compared in tabular form in [22].

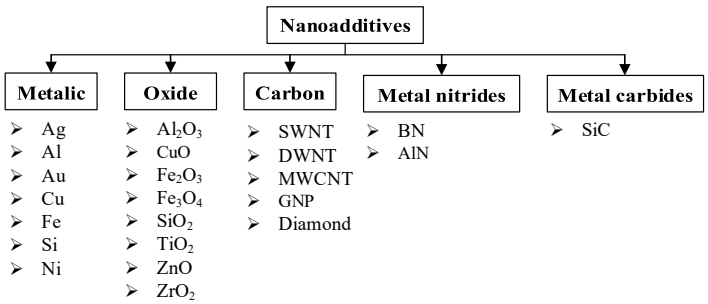

Figure 1. The types of nanoparticles most frequently used to prepare nanofluids.

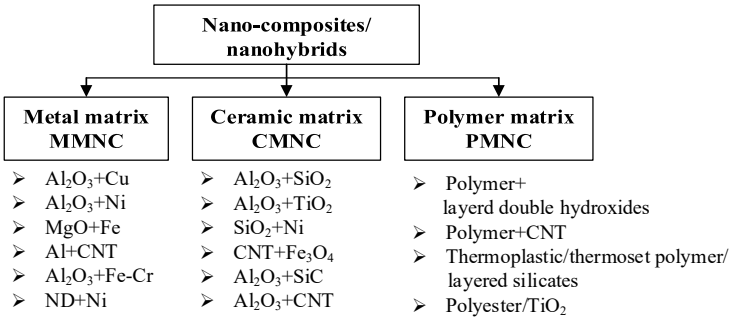

Figure 2. The types of most frequently used nanocomposites forming hybrid nanofluids [22,23].

The combination of at least two types of particles in one base fluid allows a wider range of applications due to the possibility of free modification of fluid properties. The parameters controlled first of all are the thermal conductivity of heating medium or coolant, the surface tension and the degree of hydrophobicity. Depending on the type, shape and size of the selected nanoparticles, other nanoparticle parameters including thermal diffusivity, viscosity and convective heat transfer coefficient are also modified. In this way, systems characterised by high energy efficiency are obtained for heating and cooling applications.

1.3. Ferrofluids

It is important to emphasise here the exceptional specific properties these substances show, known already in the 1960s: ferroliquids (ferrofluids or alternatively ferromagnetic, magnetic fluids and liquid magnets) [24] are classified as intelligent nanofluids because of the possibility to control their location using an external magnetic field—a magnet [25,26]—which allows keeping the liquid in a specific position in the system where it works. This property offers many options as regards to enhancement of heat transfer conditions [27] in numerous measuring systems, electronics (speakers), optical systems (for modification of the shape and properties of mirrors), and even the arms industry. They are also deemed environmentally-friendly, inexpensive and efficient—working as a sealing or lubricant (magnetic sealing) in industrial rotation equipment (such as stepper motors—reciprocating engines), and high pressure and high vacuum valves [28].

In this case, the basic fluids usually are organic solvents or water; nanodots, i.e., 10-nm (or smaller) particles of a ferromagnetic substance (e.g., magnetite) are most often used; ferroliquid stabilisation is

effected with a surfactant such as lecithin, tetramethyl ammonium hydroxide (TMAH), oleic or citric acid, which makes molecules agglomeration or sedimentation impossible. What's more, negligible conglomeration of suspension molecules results from rather strong Brownian motion, which keeps nanopowder particles homogeneously dispersed in the entire liquid volume.

1.4. Mono vs. Hybrid Nanofluids: Future Challenges

In [29] it has been shown that Ag–CuO/water hybrid nanofluid has a much higher heat transfer rate in comparison with nanofluids based on a single additive. The same conclusions were also published in [30], where (SWCNTs)/MgO-ethylene glycol hybrid and unitary nanofluids of SWCNTs and MgO were compared.

In one of the most recent works on hybrid nanofluids [22], the issues concerning their preparation, thermophysical properties, applications and challenges were discussed very broadly. Attention was also given to the need for thorough research on methods for hybrid nanofluid stabilisation and the development of correlations allowing unequivocal evaluation of the profitability of their use with reference to obtained thermophysical parameters [31]. These seem to be the primary barriers in undertaking the respective studies and popularising the use of fluids of this type in commercial systems [32].

The number of scientific studies and publications concerning the behaviour and properties of hybrid nanofluids is growing, although it still represents a slight percentage (in 2013 it was only 0.6%, and in 2017—ca. 3%) of all papers on nanofluids [22]. A thorough study analysis [33,34] allows observing the following:

- conventional models specified for mono nanofluids do not apply in the case of hybrid nanofluids; what's more there are no unequivocal experimental results or agreement regarding available models and characteristics among researchers involved in this subject,
- the relative viscosity and density of a hybrid nanofluid is directly proportional to the concentration of nanoparticles and inversely proportional to the temperature,
- thermal conductivity and heat capacity increase with temperature,
- with rising temperature and concentration of nanoparticles, the thermal properties improve until the critical point is reached—a visible deterioration of nanofluid thermal properties is observed beyond this point,
- the thermal conductivity ratio, viscosity, density, heat capacity, pressure drop and friction factor of a hybrid nanofluid are slightly higher than for the base fluid and mono nanofluid, and they grow directly proportionally to the concentration of nanoparticles,
- dispersion of nanoparticles in the base fluid is a problem frequently during stabilisation, and suspension stability time is relatively short (up to 60 days [35]),
- Brownian motion of nanoparticles and micro-convection effect, clustering and pH values strongly affect the thermal parameters of hybrid nanofluids (which is very rarely discussed in the literature) [36],
- coagulation and clustering of multi-sized nanocomposites in a nanofluid strongly affect its thermal properties [37,38],
- there are quite a few valuable papers examining from a statistical point of view of mono and hybrid nanofluid preparation, stabilization and evaporation in specific systems [39,40].

Considering the above, it becomes necessary to carry out intensive research works in order to determine the upper temperature and concentration limits for different hybrid nanoliquids working in commercial systems [22]. Moreover, it would be valuable for scientific circles to develop a general correlation, taking into account a wide range of thermodynamic parameters for all or a majority of hybrid nanofluids. It is also proposed to determine and characterise the critical point, above which a visible deterioration of nanofluids' thermal properties is observed.

A relatively short stability time is an indisputable limitation in the use of hybrid nanofluids, which also requires further studies in order to develop efficient stabilisation methods.

Special attention should also be paid to unit costs [32], as in the advanced systems, in which the working media are employed in large amounts, the use of nanoliquids may not be cost-effective. The nanoliquid preparation itself can also prove to be expensive, depending on the method chosen. What's more, the adopted method of nanofluid production and stabilisation affects its further properties as the heating or cooling medium. Various statistical design of experiment methods (DOE) are used in order to optimise nanofluid production costs while at the same time maintaining its desired thermodynamic parameters. Among these methods there are: one-factor designs, factorial designs (including general full factorial design), two level full factorial designs, two level fractional factorial designs, Plackett–Burman designs and Taguchi's orthogonal arrays [41].

Besides the purchase costs of nano-additives themselves, which are undoubtedly an obstacle in the commercialisation of nanofluid-based systems, we can also mention the time-consuming and expensive stabilisation of suspensions and problems with maintaining constant thermal properties [42] during prolonged thermal liquid use.

This paper provides a review of the basic and most common methods used for nanofluid preparation, with special attention paid to the thermal and physical properties. Moreover, an attempt has been made to systematise both the nomenclature of nanofluids and hybrid nanofluids and evaluate their stability using available methods and measuring equipment.

2. Nanofluids and Hybrid Nanofluid Symbol Suggestions

Numerous symbols are used in the literature to describe nanofluids and hybrid nanofluids, which should be both explained and standardised in order to ensure correct understanding and quick identification of a specific nanofluid. This results from rather considerable freedom, but mainly from the lack of an equivalent standardization regarding colloid preparation. Moreover, the nano-additives production stage is also characterised by diversity. Very often, a thorough study of multipage articles is required to compare or analyse thermodynamic properties of a specific suspension, which is rather labour-intensive and brings about a lot of confusion, especially in engineering applications. Although this sector of science is popular and continuously growing, it happens that laboratory analyses carried out independently for the same nanofluid frequently give quite different results. This may result from different volumes of applied nano-additives, their acquisition method, and on the other hand from the adopted stabilisation technique, or the base fluid purity. Here, summary tables prepared by researchers are very helpful, provided that their content is clear and correct [42].

Most often, the review of current knowledge on the subject shows nanofluids being identified as: Fe_3O_4/water, ZnO-EG, TiO_2/bidistilled water. The first term is the chemical formula of the nano-additive, the second identifies the base fluid. It happens that authors frequently skip the information on the base fluid, using only a symbol, e.g., CNTs. Therefore, it is proposed to add to the above symbols obligatory notation including e.g., concentration and size of nanoparticles and additionally indicating the selected stabilisation method, as shown in the Expression.

Nanoparticle (concentration, vol, %/ average nanoparticle size, nm/ nanoparticle shape)/Base fluid/Stabilization method used (i.e., two-step or more with precise sonication time and frequency data and so on.)

Here is an identification example, according to the above formula, of a single additive-based nanofluid: TiO_2 (0.1/4-8)/ DIwater/ two-step or Au ($0.6 \times 10^{-4} \div 2.6 \times 10^{-4}$/10/spherical)/DIwater/ two-step, CuO (0.016/?/nonspherical)/water/Tiron; in case of hybrid nanofluids, when the sizes of individual nanopowders are not known, averaged parameters should be specified, e.g.,: Al_2O_3+Cu (0.1–2/15/?)/DIwater/a chemical route synthesis.

Due to growing interest of the researchers in hybrid nanofluids, and their synergistic nature [43], the need to standardise their composition notation, which will facilitate comparison and practical selection for industrial applications, should be obvious.

3. Mechanisms of Nanofluids Stability

The researchers involved in an efficient use of nanofluids (including hybrid nanofluids) in technological systems agree as regards the key issues connected with their use (among them the most important are the tstabilisation duration and method) [44]. Moreover, another important issues are the costs of nanoparticle synthesis/purchase and the problems with adequate selection of particle type and the preparation of nanofluids [33], which are to work at various heat exchange ranges and different Reynolds number values [45].

Understanding the primary mechanism of particle sedimentation process as one of the phenomena that destabilise nanofluid, is crucial for developing an efficient method of stabilisation, that is, obtaining a suspension with constant properties that are maintained for as long as possible. Thus, the following forces act on a nanoparticle with density ρ_N, volume V_N and radius R_N, immersed/suspended in the base fluid with ρ_F: hydrostatic lift F_b and gravity F_g (see Figure 3) applied in opposite directions.

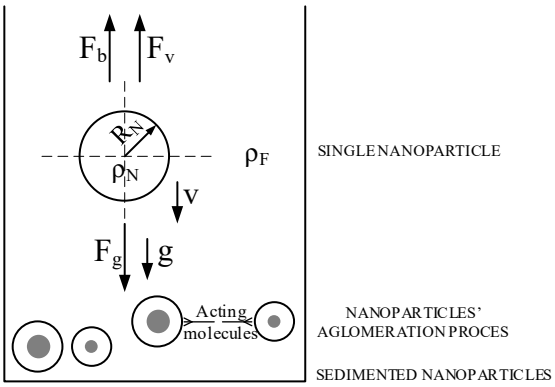

Figure 3. Distribution of forces acting on a nanoparticle immersed in fluid; ρ_N, R_N—nanoparticle characteristics suspended in the base fluid as density and radius respectively, ρ_F—base fluid density, F_b, F_g, F_v—hydrostatic, gravity and friction force respectively, v—minor velocities of dropping molecules, g—gravitational acceleration.

The particles will start falling on the bottom when $\rho_N > \rho_F$, as described by Equation (1).

$$F_g - F_b = F_{netto} = V_N(\rho_N - \rho_F)\mathrm{g} \tag{1}$$

The left hand side of Equation (1) concerns the difference between gravitational and hydrostatic forces, which is defined as F_{netto}. Under stationary conditions, $F_g = F_b$ ($v = 0$). The right hand side of Equation (1) is the ratio of nanoparticle volume, V_N, gravitational acceleration, g and the nanoparticles' and base fluid densities difference, respectively, $\rho_N - \rho_F$.

Moving molecules induce internal friction forces F_v opposite to their velocity vector and directly proportional to their size. Therefore, the force F_v compensates gravity and ensures the state of equilibrium for the molecules in liquid.

Under stationary conditions, at minor velocities of dropping molecules, v (defined as the stationary settling velocity), the friction force is directly proportional to them and depends on friction factor f:

$$F_v = v\,f \tag{2}$$

the following formula is true as well:

$$F_{netto} = F_v \tag{3}$$

$$V_N(\rho_N - \rho_F)\,\mathrm{g} = v\,f \tag{4}$$

Going further, according to thermodynamic knowledge, the weight of molecules $m_N = V_N \rho_N$, so Equation (4) can be also given as follows:

$$m_N\left(1 - \frac{\rho_F}{\rho_N}\right)\mathrm{g} = v\,f \tag{5}$$

The above indicates that in this case the shape of molecules is insignificant.

In turn, Stokes' law describes the resisting force and motion of a single spherical molecule with radius R_N in relation to the liquid surrounding it. Boundary sedimentation rate is determined on the basis of this law, Equation (6):

$$v = \frac{2}{9}\frac{{R_N}^2}{\mu}(\rho_N - \rho_F)\mathrm{g} \tag{6}$$

Therefore, radius R_N, weight, m_N and friction factor, f of a spherical molecule are defined as follows:

$$R_N = \sqrt{\frac{9\mu v}{2(\rho_N - \rho_F)\mathrm{g}}} \tag{7}$$

$$m_N = \rho_F \frac{4}{3}\pi {R_N}^3 \tag{8}$$

$$f = 6\pi\mu R_N \tag{9}$$

Equations (6)–(9) indicate that the reduction of nanoparticle size R_N and difference in densities ρ_N - ρ_F, or the increase of dynamic viscosity coefficient in the base fluid μ reduce the sedimentation rate v and contribute to improved suspension stability. It is thought that, regarding all of the methods listed above, the optimal one is nanoparticle size reduction R_N [46]. The existence of the so-called boundary rate should be pointed out here, at which sedimentation phenomenon is reduced as much as possible, and it is connected with diffusion Brownian motions of nanoparticles. However, on the other hand, smaller molecules, due to their greater surface energy, show a tendency to agglomerate. This also disturbs colloid stability, reached owing to repulsive forces compensating attractive forces in the presence of Brownian motions. Depending on the type of repulsive force, there are two mechanisms to reach colloidal stability: electrostatic and polymeric stabilization.

As far as electrostatic stabilization of colloids is concerned, it is vividly described by Derjaguin, Verway, Landau, and Overbeek theory (DVLO/sometimes DLVO), [47] according to which the stability of colloids (that include nanofluids as well) is defined by potential energy of molecules F_N, constituting the sum of potential Van der Waals attraction (attracting potential energy—Van der Waals) F_A and potential energy of the repulsive electrostatic interaction F_R (double layer of counterions), Equations (10)–(12).

$$F_N = F_A + F_R = -\frac{AR_N}{12x} + 2\pi\varepsilon\varepsilon_0 R_N Z^2 e^{-\kappa x} = \frac{64\,\mathrm{k_B}\,T\rho_\infty\,Z^2}{\kappa}e^{-kx} \tag{10}$$

$$\kappa = \sqrt{\sum_i \frac{\rho_{\infty i} e^2 z_i^2}{\varepsilon\varepsilon_0 \mathrm{k_B} T}} \tag{11}$$

$$F_N = -\frac{AR_N}{12x} + \frac{64\,\mathrm{k_B}\,T\rho_\infty\,Z^2}{\kappa}e^{-kx} \tag{12}$$

where ρ_∞ is the number density of ion in the bulk solution.

Moreover, as a formality the following is listed as well (proposed by Stokes-Einstein): particle diffusion constant (D), which strongly affects Brownian motions of spherical particles through a liquid with low Reynolds number of molecules, Equation (13):

$$D = \frac{\mathrm{k_B}T}{6\,\pi\,\mu\,R_N},\ \mathrm{m^2/s} \tag{13}$$

Diffusivity is also connected with the time required for molecules to move according to Equation (14):

$$t = \frac{2R_N}{6D} = \frac{6\,\pi\,\mu\,(2R_N)^3}{6\,k_B T} \quad (14)$$

The study [48] additionally specifies relationships defining mean free path of molecules, l MFP and time required for heat exchange τ_H. However, it is thought that these formulas do not describe unambiguously the effect of nanoparticle diffusion in the base fluid.

4. Basic and Most Common Methods of Nanofluid Preparation and Stabilization

4.1. Preparation

The first stage of the research on the properties of nanofluids used in different applications involves their preparation, that is the proper 'combining' of the base fluid with a dispersant appearing in the form of spherical or cylindrical solid particles (nanopowders/nanoadditives/ nanoparticles) sized from 1 to 100 nm. The most frequently used base fluids include: deionized water, oil [49,50], ethylene and propylene glycol, glycerol and their mixtures, e.g., water and ethylene glycol (40:60 proportion by volume) [51].

The basic problem encountered while preparing a nanofluid is how to obtain a sufficiently stable suspension to ensure that nanoparticles show no significant tendency to agglomerate over time and are evenly distributed in the entire liquid volume [52]. This difficulty results from the strong attractive Van der Waals forces acting among the molecules, which make them merge and drop on the bottom under the force of gravity, as explained before.

The most frequently applied nanoliquid preparation methods are: one-step (or bottom-up) and two-step (also known as top-down) methods (see Figure 4). Moreover, different and combined stabilization techniques are also possible for some nanomolecule types and sizes, e.g., ferroparticles. Frequently, proprietary solutions are proposed for a given type of nanofluid, including hybrid nanofluids [17].

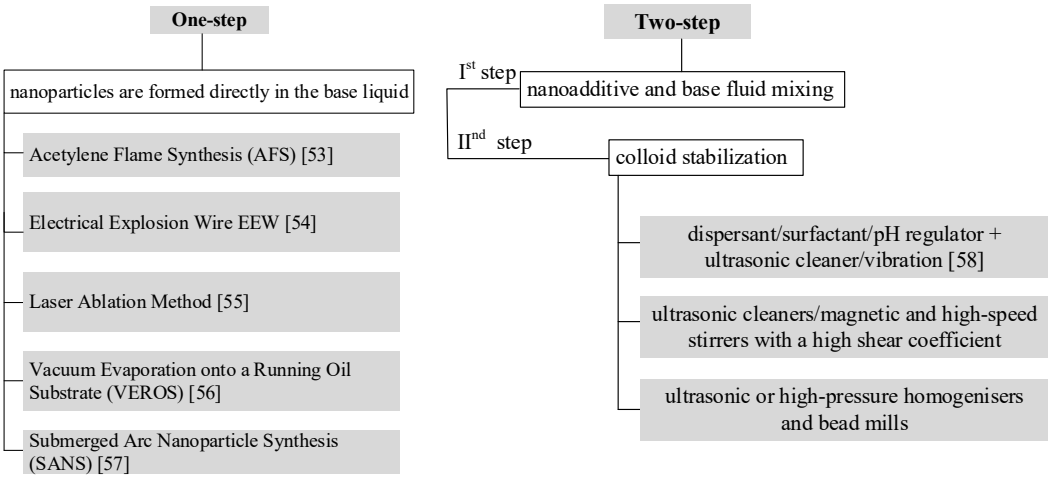

Figure 4. Basic and most common methods of nanofluid preparation: (**a**) One-step with nanoparticles formed directly in the base fluid; (**b**) Two-step concerns mixing previous fabricated nanoadditives with base fluid and stabilization of the colloid [53–58].

4.1.1. One-Step Method

In the one-step method, nanoparticles are formed directly in the base liquid [59]. Thus, the synthesis of nanoparticles and their dispersion in the base fluid proceed simultaneously, hence the process name—one-step (see Figure 5). These can be divided into two basic and independent techniques:

direct evaporation and single-stage synthesis. The first one was introduced and developed in 1978 by Akoh et al. and it is called the Vacuum Evaporation onto a Running Oil Substrate (VEROS) technique. In the literature VEROS is often modified using e.g., high pressure magnetron sputtering [60]. Another one-step method used to prepare copper-based, silver and some magnetic nanofluids is the Submerged Arc Nanoparticle Synthesis System technique (SANSS/SANS) [57]. The next one is based on the laser ablation method [55].

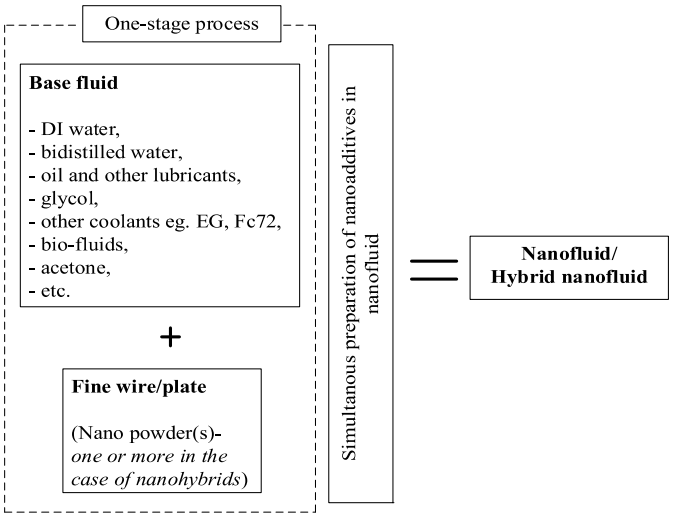

Figure 5. Block diagram of one-step nanofluid preparation method.

On the other hand, in [54], the Electrical Explosion Wire EEW technique was used to prepare a long-stability hybrid nanofluid of tungsten (III) oxide (WO_3)—silver/transformer oil. This allowed a 41% thermal conductivity improvement. Other effective one-step methods used to produce hybrid nanofluids are the acetylene flame synthesis system (AFSS) [53], or the pulsed wire evaporation (PWE) method [61] (Ag+MWCNTs/water).

The advantage of the one-step techniques is that the probability of nanoparticles agglomeration is minimal. The main disadvantage is the small scope of available liquids, which results from the vapour partial pressure limitation [62].

4.1.2. Two-Step Method

In the two-step method, a nanopowder, prepared physically or chemically, is first mixed with the base liquid using e.g., a ball mill (see Figure 6). In the second step, in order to prevent agglomeration of molecules, the liquid is exposed e.g., to ultrasound (mechanical action, especially in the case of fluids used in heating systems) or, not as often, chemical agents are added to it.

This method is preferred due to economic and quality advantages it offers [63]. However, as discussed in [64] it is more suitable for oxide than for metallic nanoparticles.

Stabilisation, i.e., the balance of attracting and repelling forces between particles suspended in the solution, is vital for the correct preparation of nanoliquids. If suitable conditions is not met, agglomeration and sedimentation of nanoparticles in the base liquid will occur. This is due to the Van der Waals forces being stronger than the forces that oppose the attraction of particles. Considering this, different optimisation methods are used to improve suspension stability, which are characterised in Section 4.2.

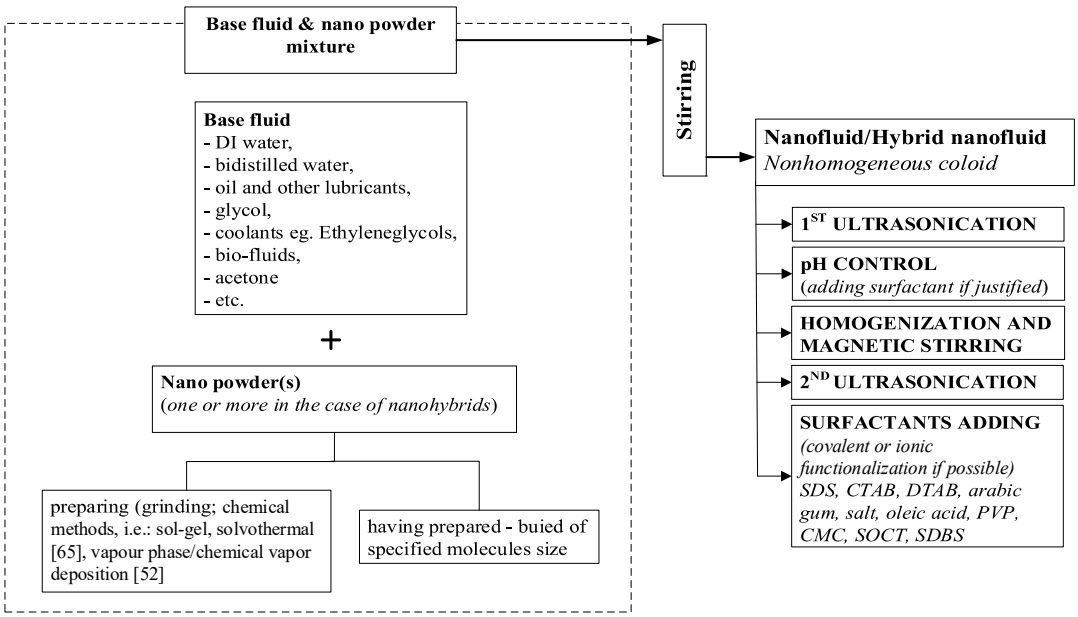

Figure 6. Block diagram of a two-step nanofluid preparation method [52,65].

The study [41] is an example of a very precise two-step preparation of a magnetite-based ferrofluid (Fe_3O_4) with 20–30 nm particle size. In the first step, nanoparticles were subjected to grinding in a mortar in order to reduce sedimentation and agglomeration. Next, the material was added to double distilled water (1% mass fraction) and mixed manually. In the second step, the suspension was put/poured into an ultrasonic cleaner (the main parameters of the process were as follows: 37 kHz, 400 W, 50 °C). Then, after setting the pH value of the obtained substance, a suitable surfactant was added and again mixed manually. Later, the suspension was put into a mixer, where the temperature at the final stage was 80 °C, washed with distilled water and exposed to iridium magnets to eliminate any undissolved surfactant that could be left. In the next step the suspension would be placed in an ultrasonic bath and exposed to a temperature of 50 °C.

Moreover, what seems to be quite problematic but sometimes omitted in scientific papers [66], is the suspension stability time. Table 2 lists the best effects of two-step synthesis process on the stability time of chosen hybrid nanofluids. As one may derive from Table 2, the dispersion of nanoparticles in the base fluid is frequently a problem during stabilisation and must be anticipated and the suspension stability time is relatively short (up to 60 days).

4.1.3. Other Methods

Nanofluid production methods can be also simply classified as mechanical, physical, chemical and combined (see Figure 7). Here, attention should be focused on a simple and low-budget physical method, the so-called electrical explosion wire method (EEW), which is sometimes used in combination with the chemical spark explosion technique [67], and is readily employed especially in case of silver particles [68]. In this system, a fluid containing metal wires of relatively high diameters is overheated, evaporated, and then transformed into a plasma state. Such operations lead to the development of nanoscale particles from metal wires exploding in the liquid. Usually these explosions need to be repeated 10 times.

Table 2. The best effects of two-step synthesis process on the stability time of chosen hybrid nanofluids.

Nanoparticles Type	Base Fluid	Particle Loading, Vol. %	Particle Size, nm	Dispersion Method (Ultrasonication, h/Magnetic Stirring, h)	Stability Time, Days	Ref.
Al_2O_3 ZnO CuO	EG/water 60:40	1–10	53 29, 0, 77.0 29	2/-	Not reported	Vajjha and Das 2009 [39]
MWCNTs-ZnO	water/EG			3/2	10	Esfe et al. 2017 [70]
Aluminum Nitride	EG	1–4	30	2.5/-	60	Hussein 2017 [50]
TiO_2/SiO_2 TiO_2:SiO_2 of 20:80, 40:60, 50:50, 60:40, 80:20	water/EG	1	50/22	2/1	14	Hamid et al. 2018 [71]
TiO_2/SiO_2	water/EG			1.5/-	14	Nabil et al. 2017 [72]
SiC-TiO_2	diathermic oil	0.1–1	30/10	2/0.5	10	Wei et al. 2017 [73]
SiO_2-graphene	naphthenic mineral oil	0.01, 0.04, 0.08		4/-	14	Qing et al. 2017 [74]
MWCNTs-Fe_2O_3	water	0, 0.1, 0.3	30/13	1/-	60	Sundar et al. 2014 [35]

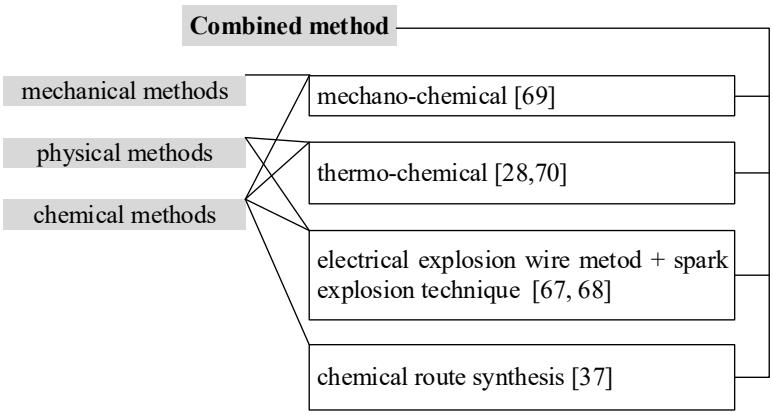

Figure 7. Block diagram of combined nanofluid preparation method [28,37,67–70].

Another example, this time regarding preparation of hybrid nanofluid, is a reported chemical-mechanical method for the synthesis of nanoparticles $Cu+Al_2O_3$ [69]. A chemical-thermal technique was employed to obtain a nanocrystalline hybrid powder, consisting of the following stages: spray-drying, oxidation, reduction in a hydrogen atmosphere and homogenization [75]. This method was also used in [28,76].

4.2. Stabilization/Nanofluids Stability Increasers

4.2.1. Surfactants

Few basic nanofluid stabilization methods can be distinguished. The simplest one seems to be adding to the suspension amphoteric, anionic, cationic, or nonionic dispersants and activators, also called promoters (e.g.,: gum Arabic, cetyltrimethyl ammonium bromide (CTAB), dodecyltrimethyl ammonium bromide (DTAB), sodium dodecylbenzene sulfonate (SDBS), dodecyl sulfate (SDS), sodium octanoate (SOCT), salt and oleic acid or polyvinyl pyrrolidone (PVP)). This method is fast, but it may affect the thermophysical properties of the system [77,78]. Especially in installations operated with changing working medium phases it is important to ensure the chemical and thermophysical stability of the system, which is connected with sought after thermodynamic parameters of the medium for specific applications. Surfactants can induce, among other effects, a reduction in the thermal conductivity of the nanofluid [79] or changes in wettability, which is confirmed by studies carried out on graphene nanoplatelets (GNPs) characterized by high thermal conductivity [80,81]. It turns out in this case that the best stabilization method is covalent functionalization [82].

4.2.2. Ultrasonication, Homogenization, Milling

Dispersion, i.e., the separation of agglomerated particles that tend to form in nanoliquids can be achieved by utilizing the following devices: ultrasonic cleaners (both bath and the probe type), magnetic and high-speed stirrers with a high shear coefficient, high shear and high-pressure homogenizers and ball mills. Moreover, sol–gel and vapor phase methods can also be used.

During the ultrasonication process supersonic waves cause the disintegration of large particles into smaller ones wherein a longer sonication time not always causes a particle size reduction and better stability [83]. In turn, high shear homogenizers use mechanical energy for breaking down the agglomerated particles whereas high-pressure homogenizers force the particles to flow through thin holes under high pressure. Both methods are very effective. As far as ball milling is concerned, there are two commonly known methods: stirred bead milling—without surfactant addition—and dry and wet ball milling—with the use of stabilization agent. As it derives from [84,85] the second way gives better and faster results but with high-temperature processes it should be used carefully.

4.2.3. pH Regulators

The pH value of a solution strongly depends on and affects its zeta (electrokinetic) potential. A typical diagram of the relationships between these values is shown in Figure 8. The point of intersection of the function with the X-axis is the so-called isoelectric point (IEP), which corresponds to a zero value of the zeta potential $\zeta = 0$ mV, for which colloidal solutions are considered the least stable. Absolute values ζ much different from IEP allow obtaining better results, which is attainable through change in the pH of the dispersed phase. Negative zeta potential values are obtained at higher solution pH, and positive ones at lower pH.

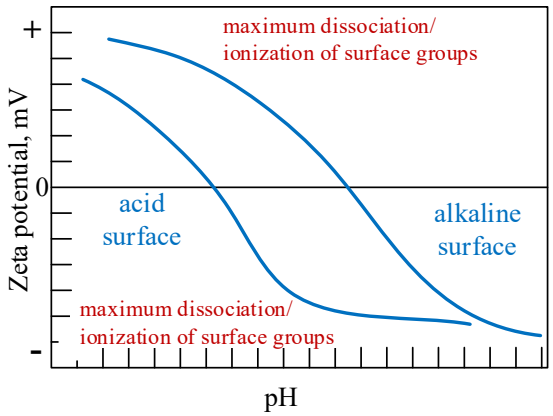

Figure 8. Electrokinetic potential in function of the pH value of a solution by Kwon [86].

Particles immersed in a solution are characterized by a specific charge density of accumulated on their surface. Acidification of the environment will cause attachment of protons (H^+ ions), and the particles will show increasing positive and decreasing negative zeta potential values. The other way, while the environment is made alkaline, the electrokinetic potential will be decreasing (hydroxy groups OH^- will be attached to particle surfaces). Therefore, during modification of the base fluid pH, electric charges on the surface of suspended particles also undergo changes, which in turn affect the suspension stability.

It is worth mentioning here the study [87], in which sulphuric acid (H_2SO_4) and nitric acid (HNO_3) were used in order to change the solvophobicity of a graphene nanoadditive (nanocomposite in hybrid nanofluid), which shows natural hydrophobic tendencies. This action aimed to improve the dispersity conditions in water solution, and thus improves its stability.

4.2.4. Steric Stabilization—Chemical Surface Alteration

Another effective method used to stabilize colloids is steric stabilization [17] as a kind of polymeric stabilization. Polymers are used in this case, which form a coating when they surround the particle, and the coating generates force repels other molecules (Figure 9). Steric repulsion can be also combined with electrostatic repulsion during stabilization and prevent aggregation processes from occurring.

This method performs well, especially when stabilizing carbon nanofluids. In this case, carbon nanotubes (CNT) are the dispersed substance. CNTs are rather widely used in industry due to their very high thermal conductivity ratio (ca. 3 kW/mK) and mechanical resistance, although due to their character (occurrence of empty structures) they are non-resistant to compressive or bending forces.

Preparation of nanofluids with added carbon nanotubes, especially multi-wall type (MWCNT), due to the way they disperse and thus also stabilize, seem to be rather problematic just due to their structure—multiple convergent tubes in one configuration, with the hydrophobic surface of these nanoadditives makes it difficult to use water as base fluid. Therefore, combined and multi-step methods are most often used during stabilization, involving ultrasonication processes, surfactants or pH regulators [88].

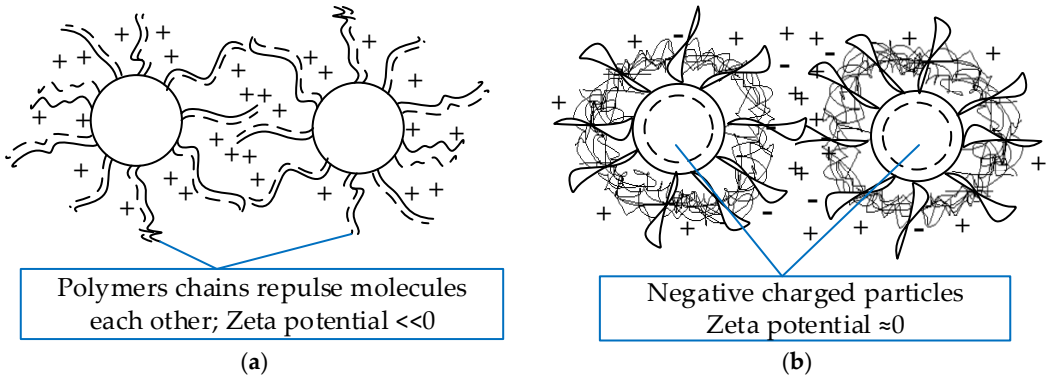

Figure 9. Polymeric stabilization of colloids (also nanofluids) should be listed as: (**a**) Steric stabilization as a physical barrier against aggregation; spatial restriction prevents molecules' agglomeration; (**b**) Electrostatic repulsion—negatively charged molecules repel each other at a short distance.

To sum up, the process of preparing stable in time nanofluids, the particles of which do not show a tendency towards significant and fast agglomeration, seems to be extremely demanding due to the need and even necessity to acquire a working medium with unchanging thermodynamic properties. It turns out that the key parameters are size and type of nanomolecules, selected base fluid (depending on the installation it is to work in) and the stabilization process itself, taking into account sonication time and intensity, the action of mixers, and selection (optionally) of surfactant. Stabilizers such as surfactants and pH regulators (electrostatic method [58,89]) have some drawbacks. It is believed that in high temperature processes stabilizers may break down, which leads to changes in liquid properties, including surface tension, wettability and viscosity [90].

5. The Quality Assessment of the Nanofluid Preparation

The following methods are used in order to perform reliable quality assessment of completed stabilization process for colloidal systems to which nanofluids may belong:

(1) Zeta potential analysis—stability characteristics of the suspension.
(2) Vibrating sample magnetometry (VSM)method—the magnetism characteristics of the suspension.

5.1. Zeta Potential Analysis

Zeta potential is determined on the verge of slipping with reference to the continuous phase potential and it is one of the determinants of stability for colloidal solutions, including nanofluids. Therefore, it is an electric potential (measured in mV) generated between dispersant (boundary outlined by the Stern layer, Figure 10), and a base fluid layer "adhering" to the molecule surface. Currently, this parameter can be determined very precisely using measuring equipment available on the market, the so-called zettameters (Zetasizer Nano ZS), which use the laser Doppler effect during the process of electrophoresis or electrophoretic dispersion of light, and Henry's equation.

As shown in Figure 10, the dispersed phase molecule contains ions adsorbed on its surface (surface charge) and a dispersed phase film containing counterions (Stern layer) adhering to the molecule owing to the electrostatic force. This is defined as an electric double layer, which is electrically neutral. It can be noted that in the direct vicinity of a molecule there is the so-called diffuse layer, which forms a dispersion medium and contains free ions with a greater concentration of counter-ions, which results from the electrostatic charge of the molecule. On the other hand, the slipping plane (or share plane) makes the boundary of the molecule move within the dispersion medium. The assessment of ferrofluid dispersion stability carried out using zeta potential measurements was applied e.g., in. [74] It was assumed there on the basis of literature data that an absolute criterial value of zeta potential, for which the suspension is deemed stable, could not be less than ζ = 20–25 mV; ζ = 40–60 mV—suspension very stable; ζ > 60—suspension perfectly stable.

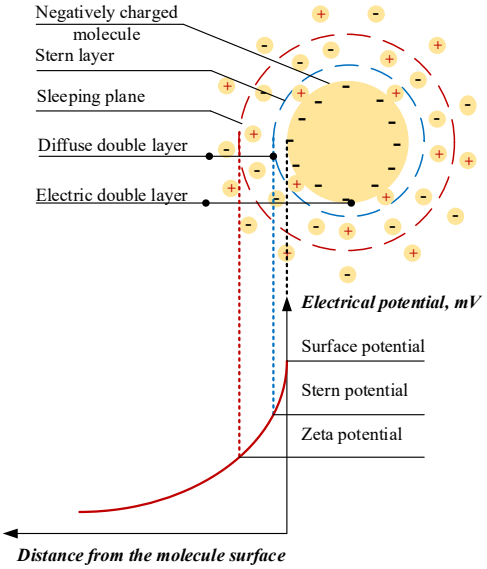

Figure 10. Electrostatic assessment of colloids stabilization. Zeta potential measurement for nanofluid particle.

In [32] it has been also shown how the zeta potential is affected by the parameters of surfactants including gum Arabic, citric acid, sodium dodecylbenzene sulfonate (SDBS), sodium dodecyl sulfate (SDS) and cetyl trimethylammonium bromide (CTAB). The following were taken into consideration: mass, heater stirring rate, v and time, t, pH, sonication times during the first t_1 and the second t_2 ultrasonication process. It turns out that the best parameters of a magnetic nanofluid, which in this case is Fe_3O_4/water, are obtained when using citric acid as surfactant, for a mixing rate and time v = 600 rpm and t = 3600 s, t_1 = 3600 s, t_2 = 1200 s, and pH = 11.

5.2. VSM Method

Besides zeta potential measurements, another method employed to evaluate the nature and stability of produced nanofluid is the VSM method using a vibrating sample magnetometer [91]. A sample is placed in the apparatus, which is then exposed to a magnetic field. The frequency of operation of electromagnetic waves is increased exponentially to the critical value. Afterwards, frequency drop is seen, which affects magnetic properties of the liquid itself. However, there is lack of proportionality observed between magnetic field intensity and magnetic properties of the sample, which is connected with magnetic anisotropy of the surroundings. If magnetic field is reduced to zero and the sample indicates magnetism residue, it proves the lack of stability and nanoparticles agglomeration tendency. Otherwise, the fluid is considered stable.

6. Nanoparticle Size Analysis

The following methods are used to analyze distribution and size of molecules in a nanofluid, following its stabilization stage:

(1) Dynamic light scattering (DLS) distribution method;
(2) Scanning electron microscopy (SEM) and transmission electron microscopy (TEM0 images;
(3) The absorption spectrum change in time (UV-Visible, use of spectrometer);
(4) X-ray diffraction (XRD)—to check molecules' crystalline structure.

The dynamic light scattering (DLS) method is also called photon correlation spectroscopy (PCS) or quasi-elastic light scattering. It is employed to determine the size of nanoparticles (also known as hydrodynamic size) and their agglomeration level in a solution as a function of time. It involves exposing a nanofluid sample to a laser beam, which is scattered by any nanoparticles present in the

solution and moving at different velocities (Brownian motions). A photon detector working with an optical correlator and software allows making the measurement and analyzing changes in light dispersion at a known angle (see Figure 11). This, in turn, makes it possible to determine the sizes of particles suspended in the solution (up to ~1 nm) according to Equation (6) (the intensity of Brownian motions depends on molecule size and translates into the rate of changes in light intensity). The DLS method is also employed to determine polydispersity index PDI (PDI = standard deviation^2/mean particle size^2) using constructive or destructive interference. If the PDI has one peak, the suspension is deemed stable. Otherwise, agglomeration of molecules should be expected in time

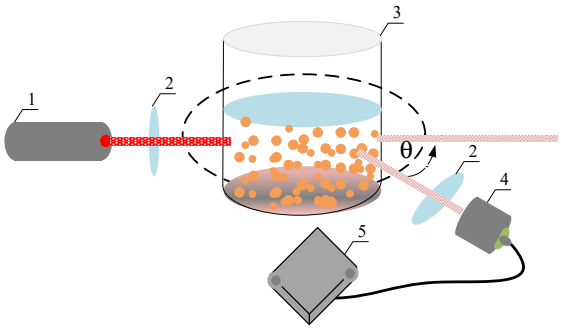

Figure 11. Example measurements of light dispersion at known angle with the use of PCS method; 1—laser, 2—lens, 3—test sample, 4—photon detector, 5—correlator.

Using both scanning and transmission electron microscopy (SEM and TEM) to determine the size and shape of nanoparticles, and the size of agglomerates formed depends on proper sample selection and preparation. In the first step it is dried, then placed on an adhesive tape, vacuum-heated and dried naturally. Afterwards, it is coated with Au and Pd, and put in a vacuum chamber, where photos are taken. Example of an analysis carried out using a scanning microscope is shown in Figure 12 and in Table 3.

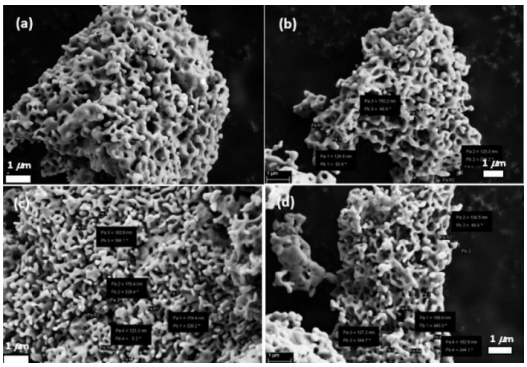

Figure 12. Exemplary pictures taken using a scanning electron microscope for: (**a**) Yttrium Iron Garnet, YIG (**b**) Lanthanum-YIG, La-YIG (**c**) Neodymium-YIG, Nd-YIG (**d**) Samarium- YIG, Sm-YIG [92].

Table 3. Weight percentage distribution of nanoparticles in four different nanofluid samples based on SEM analysis [92].

Element	Samples, Weight, %
	YIG *
Y	34.37
Fe	29.89
O	35.73
RE	0

* YIG—Yttrium Iron Garnet.

The light spectroscopy technique (UV-Vis) is used for quick assessment of nanoparticle stability in a liquid [93]. Spectrophotometers work based on this method. They measure quantitatively the degree of absorption of visible light and near ultraviolet, most often within the range from 200 to 900 nm. The intensity of light penetrating the sample I is referred to the volume of light falling onto the sample I_0. Therefore, we obtain the relationship of absorbance $A_b = log(I_0/I)$ in function of radiation wavelength, λ nm ($A_b(\lambda)$). The measurements are repeated for a few concentrations and after a few days. a drop of maximum absorbance value may indicate sedimentation of particles and suspension instability. However, this technique is inadvisable in the case of a dark-colored nanofluids or those characterized by a high viscosity coefficient, as it is, e.g., in the case of carbon nanotubes, or graphene.

Three of the abovementioned measurement techniques were used in the study reported in [67]; the X-ray diffraction, absorption spectroscopy in spectral range visible in ultraviolet (UV-Visible absorption spectroscopy), and transmission electron microscopy (TEM). Moreover, completed analyses included the impact of explosive energy volume, current voltage (charging voltage, discharge energy), wire diameter and fluid type on the size of produced nanoparticles and their distribution. The [67] presents the analysis of properties of nanofluid prepared using three base fluids (liquids): polyvinylpyrrolidone (PVP), double distilled and deionized water (DDDW), and ethylene glycol. Obtained results of the experiment correlate very well with the Lorenz-Mie theory [94] concerning determination (using optical methods) of the characteristic measure that is the particle size parameter, which depends on the wavelength of electromagnetic radiation dispersed on the surface of spherical particles with radius r (individually for other than spherical as well).

On the basis of spectroscopic tests (UV-Vis) presented in [67], it has been assessed that the produced nanoparticles of silver are spherical in shape. It has been also observed that the absorption peak has shifted to longer wavelength, and thus the liquid is instable—after 2 months nanoparticles of silver show an evident agglomeration tendency. Example analysis of results carried out using UV-Vis spectrometer is shown in Figure 13.

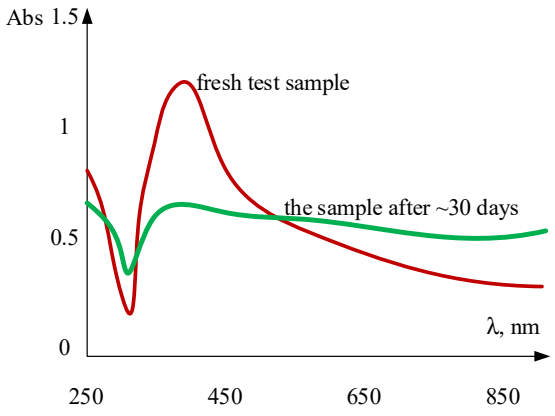

Figure 13. Exemplary UV-VIS spectrum of Ag colloid [67].

On the other hand, the TEM images show the diversity of nanoparticles within 4–81 nm (18 nm on average) and confirm the spherical shape of the molecules, indicating a slight agglomeration tendency. As far as the XRD method is concerned, it displays that Ag nanoparticles have face centered cubic structure (which is commonly abbreviated as FCCS), as it should be from the crystallographic point of view. The values of Miller's indicators, h, k, l and the grains dimension prove on puerility of the analyzed molecules. The abovementioned Miller's indicators are necessary to evaluate the lattice parameter of the synthesized nanoadditives d_{hkl} as the distance between the atom planes and as having a major influence on the diffraction peaks:

$$d_{hkl} = \frac{\alpha}{\sqrt{h^2 + k^2 + l^2}} \quad (15)$$

where α is the lattice parameter of the crystal lattice.

The computational algorithm implemented in the X-ray diffractometer uses the Debye-Scherrer formula (Equation (16)), according to which an average crystal size D_e depends on the X-ray wavelength λ, the peak width β_{pw} and Bragg's angle θ.

$$D_e = \frac{k\lambda}{\beta_{pw} \cos\theta} \tag{16}$$

where $k = 0.89$ and it is a shape factor.

The X-ray diffraction method was also used in the [35] in order to assess the crystallographic structure and phase composition of nanoadditives. Comparative results were presented there for two mono additives (MWCNT, Fe_3O_4) and for nanocomposite MWCNT + Fe_3O_4 (Figure 14). In this last case, the nanocomposite composition was confirmed on the basis of the obtained diffraction pattern. Moreover, besides a high 2θ (X-ray deflection angle) diffraction peak equal to 26 °, proving the face centered cubic structure of Fe_3O_4, no evident X-ray deflection was observed. An average size of Fe_3O_4 nanoparticles computed according to the Debye-Scherrer's formula is 13 nm. On the other hand, the SEM analysis carried out using scanning electron microscope confirmed the shape of nanoparticles. Also, Fe_3O_4 synthesis on MWCNT particles is clearly visible.

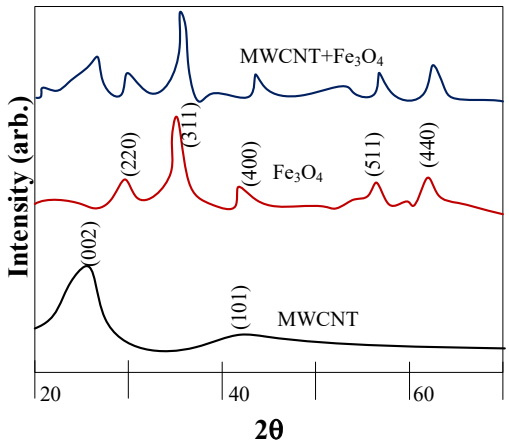

Figure 14. Exemplary X-ray Powder Diffraction (XRD) pattern of two mono nanoadditives and one nanocomposite [35].

7. Heat Transfer Enhancement

An effective improvement of heat exchange conditions due to the use of nanofluids (also or firstly hybrid nanofluids) requires their thermodynamic parameters to be controlled, first of all: thermal conductivity and other equally important values, including concentration and selection of nanoparticle type (in case of hybrids appropriate composites); preparation process itself and assessment of prepared suspension stability, or base fluid selection are important as well. Researchers agree as regards the impact of nanoadditive shape and size parameters, and formation of agglomerates (clustering effect), as well as viscosity, temperature, density, specific heat, pH and Brownian motions in the nanofluid on its thermal conductivity. However, there is no correlation between these values and the consistency of experimental studies [95]. Relationships specified in the literature do not give an unequivocal recipe for determining the thermal conductivity ratio [96].

Table 4 presents the most popular models used to determine thermal conductivity ratios for nanofluids with different concentrations and types of nanoadditives, taking into account nanocomposites as well.

Table 4. The thermal conductivity models for nanofluids most commonly specified in the literature.

Researcher	Thermal Conductivity Model	Kind of Mono/Hybrid Naofluid	Maximum Thermal Conductivity Ratio/Thermal Conductivity Increase *	Remarks
Esfe et al. 2017 [97]	$\frac{k_{nf}}{k_{bf}} = 0.905 + 0.002069fT + 0.043375f^{0.09265}T^{0.3305} - 0.0063f^3$	SiO_2+MWCNT (85:15%)/EG	22.2% for T = 50 °C	ϕ = 0.05–1.95 vol.%, T = 30–50 °C
Toghraie et al. 2016 [98]	$\frac{k_{hnf}}{k_{bf}} = 1 + 0.004503\phi^{0.8717}T^{0.7927}$	ZnO+TiO_2/EG		ϕ = 0–3.5 vol.%, T = 25–50 °C
Harandi et al. 2016 [99]	$\frac{k_{nf}}{k_{bf}} = 1 + 0.0162\phi^{0.7038}T^{0.6009}$ $TCR = \frac{k_{nf}}{k_{bf}}$ $TCE = \frac{k_{nf}-k_{bf}}{k_{bf}} \times 100$, %	MWCNTs + Fe_3O_4/EG	30% (for T = 50 °C, ϕ = 2.3%)	ϕ = 0.1, 0.25, 0.45, 0.8%, 1.25, 1.8 and 2.3 vol.%, T = 25–50 °C
Chougule and Sahu 2013 [100]	$k_{eff} = k_{bf}\left[1 + \frac{k_{p1}\phi_1 r_m}{k_m(1-(\phi_1+\phi_2))r_{p1}} + \frac{k_{p2}\phi_2 r_m}{k_m(1-(\phi_1+\phi_2))r_{p2}}\right]$			The model cannot be used for higher particle concertation.
Vajjha and Das 2009 [39]	$k_{nf} = \frac{k_p+2k_{bf}+2(k_{bf}-k_p)\phi}{k_p+2k_{bf}-(k_{bf}-k_p)\phi}k_{bf} + 5\cdot10^4\beta\phi\rho_{bf}c_{pbf}\sqrt{\frac{k_BT}{\rho_d d_d}}f(T,\phi)f(T,\phi) =$ $= \left(2.8217\cdot10^{-2}\phi + 3.917\cdot10^{-3}\right)\left(\frac{T}{T_0}\right) + \left(-3.0669\cdot10^{-2}\phi - 3.91123\cdot10^{-3}\right)$ d = 29–77 nm; T = 298-363 K; ϕ = 1–10 vol.%	Al_2O_3/EG/W, ZnO/EG/W, CuO/EG/W EG/W: 60:40	CuO/W: 1.6/60% ZnO/W: 1.49/49% Al_2O_3/W: 1.65/65%	Nanofluid thermal conductivity is directly proportional to particle concentration and temperature and inversly proportional to nanoparticle diameter
Prasher et al. 2006 [101]	$\frac{k_{eff}}{k_{bf}} = \left(1 + A\,Re^m Pr^{0.333}\phi\right)\left(\frac{\left[k_p\left(1+2Bi_p\right)+2k_{bf}\right]+2\phi\left[k_p\left(1-Bi_p\right)-k_{bf}\right]}{\left[k_p\left(1+2Bi_p\right)+2k_{bf}\right]-\phi\left[k_p\left(1-Bi_p\right)-k_{bf}\right]}\right)$ $k_{bf} = k_f[1 + 0.25Re\,Pr]; \quad A = 4\times10^4;$ $Re = \frac{1}{\nu_o}\sqrt{\frac{18k_BT}{\pi\rho d}}; \quad Bi_p = \frac{2R_{p-f}k_{bf}}{d_p}$ m = 2.5 ± (15% of 2.5) for H_2O based nanofluids, m = 1.6 ± (15% of 1.6) for EG-based nanofluids and m = 1.05 ± (15% of 1.05) for oil-based nanofluids	general H_2O, oil and EG—based nanofluids		Convective-conductive model ie. combination of Maxwell-Garnett conduction model
Chon et al. 2005 [102]	$\frac{k_{nf}}{k_{bf}} = 1 + 64.7\phi^{0.7460}\left(\frac{d_{bf}}{d_p}\right)^{0.3690}\left(\frac{k_p}{k_{bf}}\right)^{0.3690}Pr^{0.9955}Re^{1.2321}$	H_2O based nanofluids		Based on Buckingham-Pi theorem with a linear regression scheme; Brownian motion of the nanoparticle is the crucial factor in the nanofluids thermal conductivity enhancement
Yu and Choi 2003 [103]	$k_{eff} = \frac{k_p+2k_1+2(k_p-k_1)(1+\beta)^3\phi}{k_p+2k_1-(k_p-k_1)(1+\beta)^3\phi}k_1$ $\gamma = \frac{k_{layer}}{k_p}$ $\phi' = \frac{4}{3}\pi(r+h)^3 n = \frac{4}{3}\pi r^3 n\left(1+\frac{h}{r}\right)^3 = \phi(1+\beta)^3$ Based on: $k_{equiv} = \frac{\left[2(1-\gamma)+(1+\beta)^3(1+2\gamma)\right]\gamma}{-(1-\gamma)+(1+\beta)^3(1+2\gamma)}k_p$ The model is modified Maxwell model. It is noticeable that nanolayer is higher for smaller nanoparticles (r~h) It is appropriate for $h \le 5$ nm For larger particles, when h > 10 nm ($r >> h$, $\beta \to 0$), the nanolayer impact is small and [103] model reduces to the original Maxwell model	1.0 vol.% Cu/EG	8× higher value than Maxwell model without taking into account the nanolayer	Authors suggest to insert particles of smaller diameter (<10 nm) instead of adding more particles of higher diameter.
Xuan et al. 2003 [104]	$k_{nf} = \frac{k_p+2k_{bf}-2(k_{bf}-k_p)\phi}{k_p+2k_{bf}+(k_{bf}-k_p)\phi}k_{bf} + \frac{\phi\rho_p c_{pp}}{2}\sqrt{\frac{k_BT}{3\pi r\mu_{bf}}}$	Cu/W		The model includes the Brownian motion of nanoparticles, which enhances the thermal conductivity of the nanofluid.
Hamilton and Crosser 1962 [105]	$k_{eff} = \frac{k_p+(n-1)k_{bf}-(n-1)(k_p-k_{bf})\phi}{k_p+(n-1)k_{bf}+(k_{bf}-k_p)\phi}k_{bf}$			For spherical particles n = 3 and Hamilton-Crosser model is equals the Maxwell model
Maxwell 1873 [3]	$k_{Maxwell} = \frac{k_p+2k_f+2(k_p-k_f)\phi}{k_p+2k_f-(k_p-k_f)\phi}k_f$			The model does not include the nanolayer

* in comparision with pure water.

8. Conclusions

Indisputably, mono and hybrid nanofluids are a new generation of heat transfer fluids for various applications. The most important points covered by this review are:

- selection of a proper nanofluid stabilization technique,
- quality assessment of nanofluid preparation with different and available methods,
- thermal conductivity models and enhancement of heat transfer rate,
- new mono and hybrid nanofluids symbology suggestions,
- future challenges and problems need to be solved with nanofluids as the working medium.

Funding: The project financed under the program of the Minister of Science and Higher Education—'Regional Initiative of Excellence' in 2019–2022; project number 025/RID/2018/19 funding amount PLN 12000000.

Conflicts of Interest: The authors declare no conflict of interest.

Nomenclature

Greeks Latter	
α	is the lattice parameter of the crystal lattice
β_{pw}	peak width
β	the ratio of the nanolayer thickness to the original particle radius (β = h/r)
γ	interfacial thermal conductivity ratio
δ	standard deviation
ε	dielectric constant of the solvent
ε_0	vacuum permittivity
ζ	zeta potential
θ	Bragg's angle
κ	a function of the ionic concentration
λ	radiation wavelength
μ	dynamic viscosity coefficient
ν	kinematic viscosity coefficient
ρ	density
φ	concentration
Symbols	
A	Hamaker constant
Bi_p	nanoparticle Biot number
A_b	absorbance
c_p	specific heat capacity
D	diffusion constant
D_e	an average crystal size
d	diameter
d_{hkl}	lattice parameter of the synthezied nanoadditives
f	friction factor
F_N	potential energy
F_A	potential Van der Waals attraction
F_R	energy of the repulsive electrostatic interaction respectively
F_b, F_g, F_v	hydrostatic, gravity and internal friction forces respectively
g	gravitational acceleration.
h	thickness of solid-like layer (r+h—equivalent particle radius)

h, *k*, *l*	Miller's indicators
I	radiation intensity
k	thermal conductivity
k_B	the Boltzmann constant
m	mass
n	particle number per volume
Pr	the Prandtl number of the base fluid
R, *r*	radius
Re	the Brownian–Reynolds number
$R_{p\text{-}f}$	interfacial thermal resistance between nanoparticles and different fluids
T	temperature
t	time
V	volume
v	velocity
x	distance between the surfaces
Z	zeta potential
Abbreviations (major)	
BN	noron nitride
CMC	carboxymethylcellulosum
CNT	carbon nanotubes
CMNC	ceramic matrix nano composites
CTAB	cetyl trimethyl ammonium bromide
DDDW	double distilled and deionised water
DI	deionized
DLS	dynamic light scattering
DTAB	dodecyl trimethyl ammonium bromide
DWNT	double-wall nanotubes
EG	ethylene glycol
GNP	graphene nano platelets
IEP	isoelectric point
MFP	mean free path (of molecules)
MMNC	metal matrix nano composites
MWCNT	multi-wall carbon nanotubes
NaDDBS	sodium dodecylbenzenesulfonate
PDI	polydispersity index
PMNC	polymer matrix nano composites
PVP	polyvinyl pyrrolidone
SDBS	sodium dodecyl benzene sulfonate
SDS	dodecyl sulfate
SEM	scanning electron microscopy
SOCT	sodium octanoate
SWNT	single-wall nanotubes
TEM	transmission electron microscopy
TCR	thermal conductivity ratio
TCE	thermal conductivity enhancement
XRD	x-ray diffraction
VSM	vibrating sample magnetometry
W	water
Indexes	
c	cluster
eff	effective
F/f/bf	base fluid
N/nf/ hnf	nanofluid/ hybrid nanofluid
p	(nano)particles

References

1. Rostami, S.; Shahsavar, A.; Kefayati, G.; Shahsavar Goldanlou, A. Energy and exergy analysis of using turbulator in a parabolic trough solar collector filled with mesoporous silica modified with copper nanoparticles hybrid nanofluid. *Energies* **2020**, *13*, 2946. [CrossRef]
2. Taniguchi, N. On the basic concept of "nano-technology". In Proceedings of the International Conference on Production Engineering, Tokyo, Japan, 26–29 August 1974; Volume 5, Part II. pp. 8–23.
3. Maxwell, J.C. *Electricity and Magnetism*; Clarendon Press: Oxford, UK, 1873.
4. Bozorth, R.M. *Ferromagnetism*; Wiley-IEEE Press: New York, NY, USA, 1951; Van Nostrand.
5. Akoh, H.; Tsukasaki, Y.; Yatsuya, S.; Tasaki, A. Magnetic properties of ferromagnetic ultrafine particles prepared. *J. Cryst. Growth* **1978**, *45*, 495–500. [CrossRef]
6. Duncan, M.A.; Rouvray, D.H. Microclusters. *Sci. Am.* **1989**, *261*, 110–115. [CrossRef]
7. Siegel, R.W.; Eastman, J.A. A small revolution creates materials I atomic building block at a time. *Logos* **1993**, *11*, 2–7.
8. Hill, P.G.; Witting, H.; Demetri, E.P. Condensation of metal vapors during rapid expansion. *J. Heat Transf.* **1963**, *85*, 303–317. [CrossRef]
9. Andres, R.P.; Bowles, R.S.; Kolstad, J.J.; Calo, J.M. Generation of molecular clusters of controlled size. *Surf. Sci.* **1981**, *106*, 117–124. [CrossRef]
10. Brown, D.P.; Chung, J.N.; Crowe, C.T. A numerical simulation of nanocluster formation in supersonic expansion flows. *Micromechanical Syst.* **1992**, *40*, 211–225.
11. Choi, U.S.; Eastman, J.A. Enhancing thermal conductivity of fluids with nanoparticles, Developments and Applications of Non-Newtonian Flows. *J. Heat Transf.* **1995**, *66*, 99–105.
12. Khoshvaght-Aliabadi, M.; Sahamiyan, M. Performance of nanofluid flow in corrugated minichannels heat sink (CMCHS). *Energy Convers. Manag.* **2016**, *108*, 297–308. [CrossRef]
13. Wen, D.; Ding, Y. Effect of particle migration on heat transfer in suspensions of nanoparticles flowing through minichannels. *Microfluid Nanofluid* **2005**, *1*, 183–189. [CrossRef]
14. Qureshi, Z.A.; Ali, H.M.; Khushnood, S. Recent advances on thermal conductivity enhancement of phase change materials for energy storage system: A review. *Int. J. Heat Mass Transf.* **2018**, *127*, 838–856. [CrossRef]
15. Orzechowski, T.; Stokowiec, K. Quasi-stationary phase change heat transfer on a fin. FM15—Experimental Fluid Mechanics. In *EPJ Web of Conferences*; Dancova, P., Vesely, M., Eds.; EPJ Web of Conferences Series; EPD Sciences: Paris, France, 2016; Volume 114, p. 02086. [CrossRef]
16. Radomska, E.; Mika, L.; Sztekler, K. The impact of additives on the main properties of phase change materials. *Energies* **2020**, *13*, 3064. [CrossRef]
17. Benkovičová, M.; Végsö, K.; Šiffalovič, P.; Jergel, M.; Majková, E.; Luby, S.; Šatka, A. Preparation of sterically stabilized gold nanoparticles for plasmonic applications. *Chem. Pap.* **2013**, *67*, 1225–1230. [CrossRef]
18. Suhaimi, N.S.; Md Din, M.F.; Rahman, A.R.A.; Hamid, M.H.A.; Amin, N.A.M.; Zamri, W.F.H.W.; Wang, J. Optimum electrical and dielectric performance of multi-walled carbon nanotubes doped disposed transformer oil. *Energies* **2020**, *13*, 3181. [CrossRef]
19. Sekar, A.D.; Jayabalan, T.; Muthukumar, H.; Chandrasekaran, N.I.; Mohamed, S.N.; Matheswaran, M. Enhancing power generation and treatment of dairy waste water in microbial fuel cell using Cu-doped iron oxide nanoparticles decorated anode. *Energy* **2019**, *172*, 173–180. [CrossRef]
20. Sahiner, N.; Seven, F. The use of superporous p(AAc (acrylic acid)) cryogels as support for Co and Ni nanoparticle preparation and as reactor in H_2 production from sodium borohydride hydrolysis. *Energy* **2014**, *71*, 170–179. [CrossRef]
21. Karimi-Nazarabad, M.; Goharshadi, E.K.; Entezari, M.H.; Nancarrow, P. Rheological properties of the nanofluids of tungsten oxide nanoparticles in ethylene glycol and glycerol. *Microfluid Nanofluid* **2015**, *19*, 1191–1202. [CrossRef]
22. Babar, H.; Ali, H.M. Towards hybrid nanofluids: Preparation, thermophysical properties, applications, and challenges. *J. Mol. Liq.* **2019**, *281*, 598–633. [CrossRef]
23. Madhesh, D.; Parameshwaran, R.; Kalaiselvam, S. Experimental investigation on convective heat transfer and rheological characteristics of Cu-TiO2 hybrid nanofluids. *Exp. Therm. Fluid Sci.* **2014**, *52*, 104–115. [CrossRef]
24. Wang, H.; Lu, Y.; Liu, H.; Yin, Y.; Liang, J. Preparation and Application of Magnetic Nano-Solid Acid Catalyst Fe_3O_4-PDA-SO_3H. *Energies* **2020**, *13*, 1484. [CrossRef]

25. Mączka, M.; Gągor, A.; Macalik, B.; Pikul, A.; Ptak, M.; Hanuza, J. Order-disorder transition and weak ferromagnetism in the perovskite metal formate frameworks of [(CH3)(2)NH2][M(HCOO)(3)] and [(CH3)(2)ND2][M(HCOO)(3)] (M = Ni, Mn). *Inorg. Chem.* **2014**, *53*, 457–467. [CrossRef]
26. Sheikholeslami, M.; Ganji, D.D. Ferrohydrodynamic and magnetohydrodynamic effects on ferrofluid flow and convective heat transfer. *Energy* **2014**, *75*, 400–410. [CrossRef]
27. Abadeh, A.; Mohammadi, M.; Passandideh-Fard, M. Experimental investigation on heat transfer enhancement for a ferrofluid in ahelically coiled pipe under constant magnetic field. *J. Therm. Anal. Calorim.* **2018**, *135*, 1069–1079. [CrossRef]
28. Rosensweig, R.E. Magnetic fluids. *Annu. Rev. Fluid Mech.* **1987**, *19*, 437–461. [CrossRef]
29. Hayat, T.; Nadeem, S. Heat transfer enhancement with Ag-CuO/water hybrid nanofluid. *Results Phys.* **2017**, *7*, 2317–2324. [CrossRef]
30. Esfe, M.H.; Alirezaie, A.; Rejvani, M. An applicable study on the thermal conductivity of SWCNT-MgO hybryd nanofluid and price-performance analysis for energy management. *Appl. Therm. Eng.* **2017**, *111*, 1202–1210. [CrossRef]
31. Marciak-Kozłowska, J.; Kozłowski, M.; Mucha, Z. Time and energy scales for thermal properties of nanoparticles. *Mater. Sci. Forum* **2002**, *384–385*, 75–78. [CrossRef]
32. Wciślik, S. A simple economic and heat transfer analysis of the nanoparticles use. *Chem. Pap.* **2017**, *11696*, 1–7. [CrossRef]
33. Sarkar, J.; Ghosh, P.; Adil, A. A review on hybrid nanofluids: Recent research, development and applications. *Renew. Sustain. Energy Rev.* **2015**, *43*, 164–177. [CrossRef]
34. Babu, J.A.R.; Kumar, K.K.; Rao, S.S. State-of-art review on hybrid nanofluids. *Renew. Sustain. Energy Rev.* **2017**, *77*, 551–565. [CrossRef]
35. Sundar, L.S.; Singh, M.K.; Sousa, A.C.M. Enhanced heat transfer and friction factor of MWCNT-Fe3O4/water hybrid nanofluids. *Int. Commun. Heat Mass Transf.* **2014**, *52*, 73–83. [CrossRef]
36. Wu, S.; Ortiz, C.R. Experimental investigation of the effect of magnetic field on vapour absorption with LiBr-H2O nanofluid. *Energy* **2020**, *193*, 116640. [CrossRef]
37. Xiao, X.; Jia, H.; Wen, D.; Zhao, X. Thermal performance analysis of a solar energy storage unit encapsulated with HITEC salt/copper foam/nanoparticles composite. *Energy* **2020**, *192*, 116593. [CrossRef]
38. Lee, J.W.; Kang, Y.T. CO_2 absorption enhancement by Al2O3 nanoparticles in NaCl aqueous solution. *Energy* **2020**, *53*, 206–211. [CrossRef]
39. Vajjha, R.S.; Das, D.K. Experimental determination of thermal conductivity of three nanofluids and development of new correlations. *Int. J. Heat Mass Transf.* **2009**, *52*, 4675–4682. [CrossRef]
40. Zhou, Y.; Zheng, S. Multi-level uncertainty optimisation on phase change materials integrated renewable systems with hybrid ventilations and active cooling. *Energy* **2020**, *202*, 117747. [CrossRef]
41. Passandideh-Fard, A.A.M.; Maghrebi, M.J.; Mohammadi, M. Stability and magnetization of Fe3O4/water nanofluid preparation characteristics using Taguchi metod. *J. Therm. Anal. Calorim.* **2018**, *135*, 1323–1334. [CrossRef]
42. Devendiran, D.K.; Amirtham, V.A. A review on preparation, characterization, properties and applications of nanofluids. *Renew. Sustain. Energy Rev.* **2016**, *60*, 21–40. [CrossRef]
43. Guo, S.; Dong, S.; Wang, E. Gold/platinum hybrid nanoparticles supported on multiwalled carbon nanotube /silica coaxial nanocables: Preparation and application as electrocatalysts for oxygen reduction. *J. Phys. Chem. C* **2008**, *112*, 2389–2393. [CrossRef]
44. Pavlenko, A.; Koshlak, H.; Slowak, A. Stability of multiphase liquid media. *IOP C. Ser. Earth Env.* **2019**, *227*, 1–11. [CrossRef]
45. Khan, S.I.U.; Alzahrani, E.; Khan, U.; Zeb, N.; Zeb, A. On mixed convection squeezing flow of nanofluids. *Energies* **2020**, *13*, 3138. [CrossRef]
46. Dey, D.; Kumar, P.; Samantaray, S. A review of nanofluid preparation, stability, and thermo-physical properties. *Heat Transf. Asian Res.* **2017**, *46*, 1413–1442. [CrossRef]
47. Levine, S.; Dube, G.P. Interaction between two hydrophobic colloidal particles, using the approximate Debye-Huckel theory. I. General properties. *Trans. Faraday Soc.* **1940**, *35*, 1125–1141. [CrossRef]
48. Singh, P.K.; Khandelwal, D.; Sidhant, C.; Shubham, A.; Priyanshu, N.; Rasu, N.G. Nanofluid heat transfer mechanism and thermo-physical properties: A review. *IJMET* **2017**, *8*, 156–164. Available online: http://www.iaeme.com/ijmet/issues.asp?JType=IJMET&VType=8&IType=11 (accessed on 15 July 2020).

49. Cieslinski, J.T.; Ronewicz, K.; Smolen, S. Measurement of temperature-dependent viscosity and thermal conductivity of alumina and titania thermal oil nanofluids. *Arch. Thermodyn.* **2015**, *36*, 35–47. [CrossRef]
50. Hussein, A.M. Thermal performance and thermal properties of hybrid nanofluid laminar flow in a double pipe heat exchanger. *Exp. Therm. Fluid Sci.* **2017**, *88*, 37–45. [CrossRef]
51. Prakash, V.; Rai, B.; Tyagai, V.K.; Niyogi, U.K. Dispersion and characterizations of nanofluids prepared with CuO and CNT nanoparticles. *J. Indian Chem. Soc.* **2015**, *92*, 1245–1251.
52. Lamas, B.; Abreu, B.; Fonseca, A.; Martins, N.; Oliveira, M. Assessing colloidal stability of long term MWCNTs based nanofluids. *J. Colloid Interface Sci.* **2012**, *381*, 17–23. [CrossRef]
53. Hung, Y.H.; Wang, W.P.; Hsu, Y.C.; Teng, T.P. Performance evaluation of an air-cooled heat exchange system for hybrid nanofluids. *Exp. Therm. Fluid Sci.* **2017**, *81*, 43–55. [CrossRef]
54. Aberoumand, S.; Jafarimoghaddam, A. Tungsten (III) oxide (WO3)—Silver/transformer oil hybrid nanofluid: Preparation, stability, thermal conductivity and dielectric strength. *Alex. Eng. J.* **2016**, *57*, 169–174. [CrossRef]
55. Tran, P.X.; Soong, Y. Preparation of nanofluids using laser ablation in liquid technique. In Proceedings of the ASME Applied Mechanics and Material Conference 2007, Austin, TX, USA, 3–7 June 2007.
56. Akoh, H.; Tsukasaki, Y.; Yatsuya, S.; Tasaki, A. Magnetic properties of ferromagnetic ultrafine particles prepared by vacuum evaporation on running oil substrate. *J. Cryst. Growth* **1978**, *45*, 495–500. [CrossRef]
57. Loa, C.H.; Tsunga, T.T.; Lin, H.M. Preparation of silver nanofluid by the submerged arc nanoparticle synthesis system (SANSS). *J. Alloys Compd.* **2007**, *434–435*, 659–662. [CrossRef]
58. Lee, J.H.; Hwang, K.S.; Jang, S.P.; Lee, B.H.; Kim, J.H.; Choi, S.U.S.; Choi, C.J. Effective viscosities and thermal conductivities of aqueous nanofluids containing low volume concentrations of Al2O3 nanoparticles. *Int. J. Heat Mass Transf.* **2008**, *5*, 2651–2656. [CrossRef]
59. Zhu, H.; Lin, Y.; Yin, Y. A novel one-step chemical method for preparation of copper nanofluids. *Colloid Interface Sci.* **2004**, *277*, 100–103. [CrossRef]
60. Wagener, M.; Murty, B.S.; Gunther, B. Preparation of metal nanosuspensions by high pressure DC sputtering on running liquids. *Nanocrystalline Nanocomposite Mater. II* **1997**, *457*, 149–154. [CrossRef]
61. Munkhbayar, B.; Tanshen, M.R.; Jeoun, J.; Chung, H.; Jeong, H. Surfactant-free dispersion of silver nanoparticles into MWCNT-aqueous nanofluids prepared by one-step technique and their thermal characteristics. *Ceram. Int.* **2013**, *39*, 6415–6425. [CrossRef]
62. Mukherjee, S.; Paria, S. Preparation and Stability of Nanofluids—A Review. *J. Mech. Civ. Eng.* **2013**, *9*, 63–69. [CrossRef]
63. Mali, S.; Pise, A.; Acharya, A. Review on flow boiling heat transfer enhancement with nanofluids. *IOSR J. Mech. Civ. Eng.* **2014**, *11*, 43–48. [CrossRef]
64. Wang, X.Q.; Mujumdar, A.S. A review on nanofluids part II: Experiments and applications. *Braz. J. Chem. Eng.* **2008**, *25*, 631–648. [CrossRef]
65. Syam, S.L.; Venkata, R.E.; Singh, M.K.; DeSousa, A.C.M. Viscosity of low volume concentrations of magnetic Fe3O4 nanoparticles dispersedin ethylene glycol and water mixture. *Chem. Phys. Lett.* **2012**, *554*, 236–242. [CrossRef]
66. Jama, M.; Singh, T.; Gamaleldin, S.M.; Koc, M.; Samara, A.; Isaifan, R.J.; Atieh, M.A. Critical Review on Nanofluids: Preparation, Characterization, and Applications. *J. Nanomater.* **2016**, *2016*, 6717624. [CrossRef]
67. Kadhim, S.; Humud, H.; Abdulmajeed, I.M. Silver nanofluids prepared by pulse exploding wire. *AARJMD* **2014**, *1*, 2319–2801.
68. Cho, C.; Kang, C.; Ha, Y.C.; Jin, T.S.; Rim, G.H. Optimum discharge conditions for smaller particles from Ag wire explosion in liquid media. *J. Phys. Soc. Jpn.* **2011**, *59*, 3662–3665. [CrossRef]
69. Shehata, F.; Abdelhameed, M.; Fathy, A.; Elmahdy, M. Preparation and characteristics of Cu-Al_2O_3 Nanocomposite. *Open J. Met.* **2011**, *1*, 25–33. [CrossRef]
70. Esfe, M.H.; Esfandeh, S.; Saedodin, S.; Rostamian, H. Experimental evaluation, sensitivity analyzation and ANN modeling of thermal conductivity of ZnO-MWCNT/EG-water hybrid nanofluid for engineering applications. *Appl. Therm. Eng.* **2017**, *125*, 673–685. [CrossRef]
71. Hamid, K.A.; Azmi, W.H.; Nabil, M.F.; Mamat, R. Experimental investigation of nanoparticle mixture ratios on TiO2-SiO2 nanofluids heat transfer performance under turbulent flow. *Int. J. Heat Mass Transf.* **2018**, *118*, 617–627. [CrossRef]

72. Nabil, M.F.; Azmi, W.H.; Hamid, K.A.; Mamat, R.; Hagos, F.Y. An experimental study on the thermal conductivity and dynamic viscosity of TiO2-SiO2 nanofluids in water: Ethylene glycol mixture. *Int. Commun. Heat Mass Transf.* **2017**, *86*, 181–189. [CrossRef]
73. Wei, B.; Zou, C.; Yuan, X.; Li, X. Thermo-physical property evaluation of diathermic oil based hybrid nanofluids for heat transfer applications. *Int. J. Heat Mass Transf.* **2017**, *107*, 281–287. [CrossRef]
74. Qing, S.H.; Rashmi, W.; Khalid, M.; Gupta, T.C.S.M.; Nabipoor, M.; Hajibeigy, M.T. Thermal conductivity and electrical properties of Hybrid SiO_2-graphene naphthenic mineral oil nanofluid as potential transformer oil. *Mater. Res. Express.* **2017**, *4*, 015504. [CrossRef]
75. Shehata, F.; Fathy, A.; Abdelhameed, M.; Moustafa, S. Preparation and properties of Al_2O_3 nanoparticle reinforced copper matrix composites by insitu processing. *Mater. Des.* **2009**, *30*, 2756–2762. [CrossRef]
76. Colangelo, G.; Favale, E.; Miglietta, P.; Milanese, M.; de Risi, A. Thermal conductivity, viscosity and stability of Al2O3-diathermic oil nanofluids for solar energy systems. *Energy* **2016**, *95*, 124–136. [CrossRef]
77. Rabienataj Darzi, A.A.; Farhadi, M.; Sedighi, K.; Shafaghat, R.; Zabihi, K. Experimental investigation of turbulent heat transfer and flow characteristics of SiO_2/water nanofluid within helically corrugated tubes. *Int. Commun. Heat Mass Transf.* **2012**, *39*, 1425–1434. [CrossRef]
78. Setia, H.; Gupta, R.; Wanchoo, R. Stability of nanofluids. *Mater. Sci. Forum* **2013**, *757*, 139–149. [CrossRef]
79. Zhou, M.Z.; Xia, G.D.; Li, J.; Chai, L.; Zhou, L.J. Analysis of factors influencing thermal conductivity and viscosity in different kinds of surfactant solutions. *Exp. Therm. Fluid Sci.* **2012**, *36*, 22–29.
80. Sarsam, W.S.; Amiri, A.; Kazi, S.N.; Badarudin, A. Stability and thermo-physical properties of non-covalently functionalized graphene nanoplatelets. *Energy Convers. Manag.* **2016**, *116*, 101–111. [CrossRef]
81. Sarsam, W.S.; Amiri, A.; Zubir, M.N.M.; Yarmand, H.; Kazi, S.N.; Badarudin, A. Stability and thermo-physical properties of water-based nano-fluids containing triethanolamine-treated graphene nanoplatelets with different specific surface. *Colloids Surf. A* **2016**, *500*, 17–31. [CrossRef]
82. Brinkman, H.C. The viscosity of concentrated suspensions and solutions. *J. Chem. Phys.* **1952**, *20*, 571–581. [CrossRef]
83. Chung, S.J.; Leonard, J.P.; Nettleship, I.; Lee, J.K.; Soong, Y.; Martello, D.V.; Chyu, M.K. Characterization of ZnO nanoparticle suspension in water: Effectiveness of ultrasonic dispersion. *Powder Tech.* **2009**, *194*, 1–2, 75–80. [CrossRef]
84. Silambarasan, M.; Manikandan, S.; Rajan, K.S. Viscosity and thermal conductivity of dispersions of sub-micron TiO_2 particles in water prepared by stirred bead milling and ultrasonication. *Int. J. Heat Mass Transf.* **2012**, *55*, 7991–8002. [CrossRef]
85. Yarmand, H.; Gharehkhani, S.; Shirazi, S.F.S.; Goodarzi, M.; Amiri, A.; Sarsam, W.S.; Alehashem, M.S.; Dahari, M.; Kazi, S.N. Study of synthesis, stability and thermo-physical properties of graphene nanoplatelet/platinum hybrid nanofluid. *Int. Commun. Heat Mass Transf.* **2016**, *77*, 15–21. [CrossRef]
86. Kwon, D.; Kim, H.; Leong, H. Heat and its effects to chemical mechanical polishing. *J. Mater. Process. Technol.* **2006**, *178*, 82–87. [CrossRef]
87. Yarmand, H.; Gharehkhani, S.; Ahmadi, G.; Shirazi, S.F.S.; Baradaran, S.; Montazer, E.; Zubir, M.N.M.; Alehashem, M.S.; Kazi, S.N.; Dahari, M. Graphene nanoplatelets-silver hybrid nanofluids for enhanced heat transfer. *Energy Convers. Manag.* **2015**, *100*, 419–428. [CrossRef]
88. Zhang, P.; Hong, W.; Wu, J.F.; Liu, G.Z.; Xiao, J.; Chen, Z.B.; Cheng, H.B. Effect of surface modification on the suspension stability and thermal conductivity of carbon nanotubes nanofluids. *Energy Procedia* **2015**, *69*, 699–705. [CrossRef]
89. Singh, P.K.; Harikrishna, P.V.; Sundararajan, T.; Das, S.K. Experimental and numerical investigation into the hydrodynamics of nanofluids in microchannels. *Exp. Therm. Fluid Sci.* **2012**, *42*, 174–186. [CrossRef]
90. Uskokovic, V. Nanotechnologies: What we do not know. *Technol. Soc.* **2007**, *29*, 43–61. [CrossRef]
91. Odenbach, S. Ferrofluids: Magnetically controllable fluids and their applications. In *Lecture Notes in Physics*; Springer: Bremen, Germany, 2002; Volume 594, pp. 33–58. [CrossRef]
92. Lau, Z.Y.; Lee, K.C.; Soleimani, H.; Beh, H.G. Experimental study of electromagnetic-assisted rare-earth doped yttrium iron garnet (YIG) nanofluids on wettability and interfacial tension alteration. *Energies* **2019**, *12*, 3806. [CrossRef]
93. Sadeghi, R.; Etemad, S.G.; Keshavarzi, E.; Haghshenasfard, M. Investigation of alumina nanofluid stability by UV-vis spectrum. *Microfluid Nanofluid* **2015**, *18*, 1023–1030. [CrossRef]

94. West, J.; Sears, J.; Smith, S.; Carter, M. Photonic sintering—An example: Photonic curing of silver nanoparticles. In *Sintering of Advanced Materials—Fundamentals and Processes*; Woodhead Publishing: Oxford, UK, 2010; pp. 275–288.
95. Tiwari, K.A.; Ghosh, P.; Sarkar, J. Investigation of thermal Conductivity and viscosity of Nanofluids. *J. Environ. Res. Dev.* **2012**, *2*, 768–777.
96. Özerinç, S.; Kakaç, S.; Yazicioglu, A.G. Enhanced thermal conductivity of nanofluids: A state-of-the-art review. *Microfluid Nanofluid* **2010**, *8*, 145–170. [CrossRef]
97. Esfe, M.H.; Behbahani, P.M.; Arani, A.A.A.; Sarlak, M.R. Thermal conductivity enhancement of SiO_2-MWCNT (85:15%)-EG hybrid nanofluids. *J. Therm. Anal. Calorim.* **2017**, *128*, 249–258. [CrossRef]
98. Toghraie, D.; Chaharsoghi, V.A.; Afrand, M. Measurement of thermal conductivity of ZnO-TiO_2/EG hybrid nanofluid. *J. Therm. Anal. Calorim.* **2016**, *125*, 527–535. [CrossRef]
99. Harandi, S.S.; Karimipour, A.; Afrand, M.; Akbari, M.; D'Orazio, A. An experimental study on thermal conductivity of F-MWCNTs-Fe3O4/EG hybrid nanofluid: Effects of temperature and concentration. *Int. Commun. Heat Mass Transf.* **2016**, *76*, 171–177. [CrossRef]
100. Chougule, S.S.; Sahu, S.K. Comparative study on heat transfer enhancement of low volume concentration of al2o3–water and carbon nanotube–water nanofluids in laminar regime using helical screw tape inserts. *J. Nanotechnol. Eng. Med.* **2013**, *4*, 040904. [CrossRef]
101. Prasher, R.; Bhattacharya, P.; Phelan, P.E. Brownian-motion-based convective-conductive model for the effective thermal conductivity of nanofluids. *J. Heat Transf.* **2006**, *128*, 588–595. [CrossRef]
102. Chon, C.H.; Kihm, K.D.; Lee, S.P.; Choi, S.U.S. Empirical correlation finding the role of temperature and particle size for nanofluid (Al_2O_3) thermal conductivity enhancement. *Appl. Phys. Lett.* **2005**, *87*, 153107. [CrossRef]
103. Yu, W.; Choi, S.U.S. The role of interfacial layers in the enhanced thermal conductivity of nanofluids: A renovated Maxwell model. *J. Nanopart. Res.* **2003**, *5*, 167–171. [CrossRef]
104. Xuan, Y.; Li, Q.; Hu, W. Aggression structure and thermal conductivity of nanofluids. *Am. Inst. Chem. Eng.* **2003**, *49*, 1038–1043. [CrossRef]
105. Hamilton, R.; Crosser, O. Thermal conductivity of heterogeneous two component systems. *Ind. Eng. Chem. Fundam.* **1962**, *125*, 187–191. [CrossRef]